Pure Appl. Chem., Vol. 74, No. 10, pp. 1831–1841, 2002.

Solubility equilibria. From data optimization to process simulation*

Erich Königsberger

Department of Chemistry, Division of Science and Engineering, Murdoch University, Murdoch, WA 6150, Australia

Abstract: Models that accurately predict solid–solute phase equilibria in aqueous electrolyte solutions are of mounting importance for numerous industrial processes, especially those operating at high temperatures, pressures, and concentrations. The incorporation of such electrolyte models into process simulators is in great demand. This communication will focus on thermodynamically consistent models that can simultaneously predict densities, heat capacities, and apparent molar enthalpies of multicomponent electrolyte mixtures together with activities of their constituents. Data optimization issues to be discussed include the CALPHAD (CALculation of PHAse Diagrams) method applied to electrolyte systems and the generation of robust models that extrapolate well outside the parameterization space. Recent development of software suitable for the simulation of industrial processes involving concentrated electrolyte solutions will be outlined.

INTRODUCTION

By definition, electrolyte solutions take part in all hydrometallurgical processes. It should be recalled that the electrolyte solutions in many of these processes are (a) highly concentrated, (b) mixed, and (c) hot. It should also be recalled that, so far, there are no fundamental theories that permit the calculation of the thermodynamic properties of such electrolyte solutions from first principles. Thus, purely empirical electrolyte models have often been used in the industrial context. Such models are usually thermodynamically inconsistent; i.e., separate models describe properties like densities, heat capacities, or solubilities independently of each other. Often, these models are only valid for rather narrow ranges of conditions. This kind of approach makes it virtually impossible to simulate other process variants operating at different conditions.

The incorporation in process simulators of thermodynamically consistent electrolyte models, which are valid over the entire range of temperature, pressure, and composition of interest, is therefore in great demand. These are usually semi-empirical models based on Gibbs energies, so that phase equilibria and thermodynamic properties can be calculated by appropriate differentiation performed by Gibbs energy minimizers. Among such routines, ChemSage [1] and F*A*C*T [2] are very suitable for thermodynamic calculations on electrolytes. ChemSage also contains an optimizer for the adjustment of model parameters with respect to experimental data [3]. Other programs in the ChemSage family include ChemApp [4] (a programmer's library consisting of a comprehensive set of subroutines that permits the calculation of complex, multicomponent, multiphase chemical equilibria and their associated extensive property balances) and ChemSheet [5] (a Microsoft Excel/ChemApp interface for thermodynamic process simulation). All these programs have been used in this work.

*Lecture presented at the 10th International Symposium on Solubility Phenomena, Varna, Bulgaria, 22–26 July 2002. Other lectures are published in this issue, pp. 1785–1920.

Within the thermodynamics of chemical systems, the Gibbs energy, G, is an especially important quantity. First, it is a function of the most convenient set of independent variables, temperature, T, pressure, P, and the amounts, n_i, of the chemical substances in the system. Secondly, it is directly related to the equilibrium constants of chemical reactions in the system. Thirdly, at chemical or phase equilibrium in homogeneous (single-phase) or heterogeneous (multi-phase) systems respectively, it assumes a minimum with respect to the compositional variables. The second and third of these statements are mathematically equivalent.

In the CALPHAD method, Gibbs energies of the individual phases are evaluated as functions of temperature, pressure, and composition with respect to various kinds of experimental information (phase equilibria, activities, enthalpies, heat capacities, densities, etc.). Using optimization routines, parameters of the various models are adjusted so that they describe the excess properties of the various nonideal phases as closely as possible. Since quaternary interactions are generally negligible, the optimizations are performed on binary and ternary systems in order to correlate their thermodynamic properties, with the effect that the model equations can then be used to predict the thermodynamic properties of multicomponent systems. Although originally developed by Kaufman and others (e.g., [6]) to perform equilibrium calculations on heterogeneous, high-temperature systems involving phases like alloys, slags, oxides, or silicates, the CALPHAD method has been applied to electrolyte systems as well. The literature on this subject has been reviewed recently [7].

The semi-empirical ion-interaction model developed by Pitzer [8] has convincingly demonstrated a capability to correlate, in a thermodynamically consistent way, the properties of electrolyte solutions within the experimental uncertainty of high-precision measurements over wide ranges of temperatures, pressures, and concentrations up to saturation. However, despite its success, the Pitzer model has severe limitations, as extrapolations outside the parameterization space are usually poor. These issues have been addressed in a recent review [7] and will be further investigated in this communication.

PARAMETER OPTIMIZATION

The ChemSage optimizer [3] employs a Bayes algorithm to derive model parameters with respect to a variety of experimental data. In this method, the objective function consists of two parts: the weighted sums of squares of the differences (i) between experimental data and calculated values and (ii) between calculated and so-called a priori parameters. The latter may be known from previous experiments or theoretical considerations. Thus, the two parts of the objective functions can be weighted independently, depending on whether more confidence is placed in the new measurements or the original model parameters. When no a priori information on the parameters is available, then the sum (ii) vanishes and the Bayes algorithm becomes equivalent to the standard least squares method. The ChemSage optimizer also calculates uncertainties and correlation coefficients of parameters.

The ChemSage optimizer is capable of adjusting Pitzer parameters for electrolytes with respect to the following kinds of experimental data:

- osmotic coefficients and water activities;
- relative apparent molar enthalpies, enthalpies of dilution [3,7];
- (apparent molar) heat capacities [9,10]; and
- densities and (apparent) molar volumes [3,9].

HIGH-TEMPERATURE THERMODYNAMICS OF ELECTROLYTES

Standard partial molar heat capacities and volumes

The standard partial molar quantities of electrolytes show a characteristic temperature dependence (Fig. 1a). The rapid change in C_p° as the temperature approaches 300 °C can be qualitatively explained in terms of electrostatic interactions using the simple Born expression [13]. The behavior originates

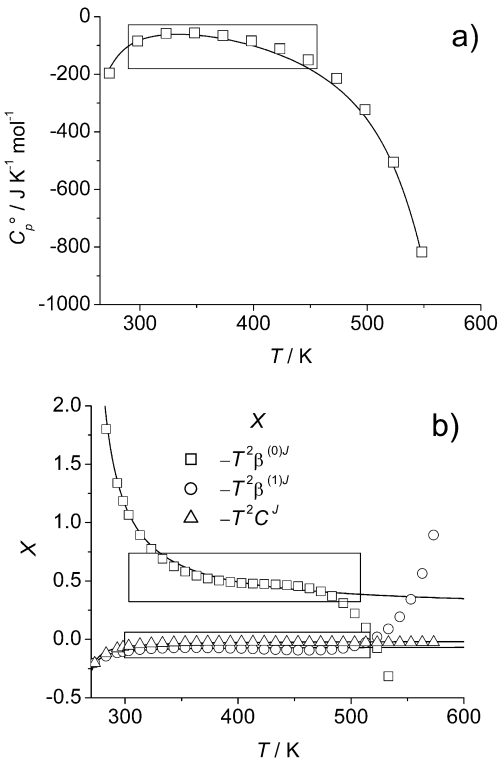

Fig. 1 (a) Standard partial molar heat capacity of NaCl(aq) at 1 bar or saturation pressure. Line [11]; squares, calculated with SUPCRT92 [12]. (b) Squares, circles, and triangles, Pitzer parameters for apparent molar heat capacities of NaCl(aq) at 1 bar or saturation pressure [11], multiplied by $-T^2$; lines, calculated according to eq. 10. In both cases, the boxes indicate the temperature ranges in which the quantities are reasonably constant.

from the strong temperature dependence of the first and second temperature derivatives of the dielectric constant of water.

While numerous *correlative* equations have been proposed for partial molar quantities at infinite dilution (see below), the revised equations of Helgeson, Kirkham, and Flowers (HKF), as embodied in the SUPCRT92 software [12], are the best known and most comprehensive *predictive* equations for these properties. For well-studied systems like NaCl(aq), the agreement between experiment and HKF prediction is very good (Fig. 1a), whereas the accuracy of the HKF predictions cannot, of course, be verified when high-temperature data are lacking. Recently, Sedlbauer et al. have proposed a new predictive expression for partial molar volumes of nonelectrolytes at infinite solution that is based on fluctuation solution theory [14].

Excess Gibbs energies

The Pitzer equations are the best-known and most precise thermodynamically consistent *correlative* equations for excess thermodynamic quantities of aqueous electrolytes. However, their *predictive* capabilities in terms of extrapolations outside the parameterization space are rather poor. Pitzer parameters do not have a fundamental temperature or pressure dependence. Moreover, Pitzer parameters are strongly correlated (statistically), so that it is not very useful to report their uncertainties without information on the correlation [15]. Consequently, different sets of parameters may describe the data used

for parameterization equally well, however, extrapolations to higher concentrations generally lead to different results.

About two dozen electrolytes have been experimentally studied over wider temperature, pressure, and concentration ranges. Various temperature functions have been proposed for the Pitzer parameters derived in these studies, one of them is the following equation [11]

$$X(T) = w_1 + w_2(T/\mathrm{K})^{-1} + w_3 \ln(T/\mathrm{K}) + w_4(T/\mathrm{K}) + w_5(T/\mathrm{K})^2 + w_6(680 - T/\mathrm{K})^{-1} + w_7(T/\mathrm{K} - 227)^{-1}. \quad (1)$$

Equation 1 has also been used [11] for standard partial molar quantities (Fig. 1a).

For most electrolytes studied to date, high-temperature data are lacking and Pitzer parameters for osmotic and activity coefficients, apparent molar enthalpies and heat capacities, are only available at 25 °C. This has led the present author to investigate various methods to extrapolate these 25 °C data to higher temperatures [7]. The so-called *constant heat capacity model* (hereafter referred to as the *CHC model*) has proven promising and will be further investigated here.

Constant heat capacity model

The Pitzer equations for excess Gibbs energies, relative apparent molar enthalpies, and apparent molar heat capacities have been reviewed many times (e.g., [7,8]), so only the essential points are mentioned here. The excess Gibbs energy of a binary electrolyte is given by

$$G^{\mathrm{E}}/(w_{\mathrm{w}}RT) = -A_\phi\,(4I\,b^{-1}) \ln(1 + bI^{1/2}) + 2\nu_{\mathrm{M}}\nu_{\mathrm{X}}\,[m^2 B_{\mathrm{MX}} + m^3 \nu_{\mathrm{M}} z_{\mathrm{M}} C_{\mathrm{MX}}] \quad (2)$$

In eq. 2, w_{w} is the mass of the solvent, m is the molality of the solute, I is the molality-based ionic strength, A_ϕ is the Debye–Hückel coefficient for the osmotic function (at 25 °C, A_ϕ = 0.3915 $\mathrm{kg}^{1/2}\,\mathrm{mol}^{-1/2}$ [16]), ν_i and z_i are the stoichiometric coefficient and the formal charge of the ion i, respectively. The temperature-independent constant b equals 1.2 for all solutes. B_{MX} is an ionic strength-dependent function of three adjustable parameters $\beta^{(0)}{}_{\mathrm{MX}}$, $\beta^{(1)}{}_{\mathrm{MX}}$, and $\beta^{(2)}{}_{\mathrm{MX}}$ (the latter is only needed for 2-2 and higher electrolytes), while in the original Pitzer equations C_{MX} is an ionic strength independent parameter.

Standard thermodynamic procedures yield the expression for the apparent molar heat capacity

$$^{\phi}C_p = (C_p - n_1\,C_{p1}{}^\circ)/n_2 = C_{p2}{}^\circ - T^2\{\partial^2(G^{\mathrm{E}}/T)/\partial T^2 + (2/T)[\partial(G^{\mathrm{E}}/T)/\partial T]\}_{P,m}/(w_{\mathrm{w}}m) \quad (3)$$

In eq. 3, $C_{p\mathrm{i}}{}^\circ$ is the standard partial molar heat capacity of component i, (the indices 1 and 2 denote solvent and solute, respectively). Applying eq. 3 to eq. 2 results in

$$^{\phi}C_p = C_{p2}{}^\circ + \nu|z_{\mathrm{M}}z_{\mathrm{X}}|\,A_J\,(2b)^{-1} \ln(1 + bI^{1/2}) - 2\nu_{\mathrm{M}}\nu_{\mathrm{X}}RT^2[mB^J{}_{\mathrm{MX}} + m^2\nu_{\mathrm{M}}z_{\mathrm{M}}C^J{}_{\mathrm{MX}}], \quad (4)$$

where

$$B^J{}_{\mathrm{MX}} = (\partial^2 B_{\mathrm{MX}}/\partial T^2)_{P,m} + (2/T)\,(\partial B_{\mathrm{MX}}/\partial T)_{P,m}, \text{ so that} \quad (5)$$

$$\beta^{(\mathrm{i})J}{}_{\mathrm{MX}} = (\partial^2 \beta^{(\mathrm{i})}{}_{\mathrm{MX}}/\partial T^2)_P + (2/T)\,(\partial \beta^{(\mathrm{i})}{}_{\mathrm{MX}}/\partial T)_P, \text{ for } i = 0, 1, 2, \text{ and} \quad (6)$$

$$C^J{}_{\mathrm{MX}} = (\partial^2 C_{\mathrm{MX}}/\partial T^2)_P + (2/T)\,(\partial C_{\mathrm{MX}}/\partial T)_P \quad (7)$$

In eq. 4, A_J is the Debye–Hückel coefficient for heat capacity, which has the value A_J/R = 3.94 $\mathrm{kg}^{1/2}\,\mathrm{mol}^{-1/2}$ at 25 °C [16].

It can be seen from eq. 4 that CHCs (apart from the variation with temperature of A_J) ensue when (i) $C_{p2}{}^\circ$ and (ii) $T^2X^J{}_{\mathrm{MX}}$ are temperature independent ($X^J{}_{\mathrm{MX}}$ denotes any Pitzer heat capacity parameter defined by eqs. 6–7).

Figures 1a and 1b show that for NaCl(aq) [11], these quantities are indeed essentially constant over wide ranges of temperature. The CHC model [7] thus seems to be a very reasonable approxima-

tion. In this model, the temperature dependence of a Pitzer parameter is given by (the logarithmic term ensues when the heat capacity is assumed constant)

$$X(T) = X_0 + a(1/T - 1/T_0) + b \ln(T/T_0). \quad (8)$$

In eq. 8, *X(T)* denotes the interaction parameter at temperature T, X_0 is its value at T_0 = 298.15 K, $a = X^J {T_0}^3 - X^L {T_0}^2$, and $b = X^J {T_0}^2$. The constants a and b are expressed in terms of enthalpy and heat capacity parameter values valid at T_0, which are denoted as X^L and X^J, respectively. If there are no heat capacity parameters available, it is further assumed that $X^J = 0$ and thus $a = -X^L {T_0}^2$ and $b = 0$. Quite frequently, only X_0 parameters have been reported and neither X^L nor X^J are available. Then, eq. 8 would result in $X(T) = X_0$, i.e., the contribution of X_0 to the excess Gibbs energy would be purely entropic [as $X(T)$ appears in the expression for G^E/RT], whereas it would usually be expected to be solely enthalpic. Thus, in this case, the convention used in the F*A*C*T database [2,17] is introduced, namely that $a = X_0 T_0$ by definition, so that

$$X(T) = X_0 T_0/T, \text{ only if } X^L = X^J = 0. \quad (9)$$

It has been demonstrated [7] that the CHC model is capable of predicting the ionic product of water in 0–6 mol kg^{-1} NaCl(aq) to 250 °C, the phase diagrams of NaCl–H_2O and Na_2CO_3–H_2O to at least 100 °C and relative apparent molar enthalpies for these two systems to about 60 °C.

Beyond the constant heat capacity model

A close inspection of Fig. 1b reveals that at low temperatures, the Pitzer parameters for apparent molar heat capacity change rapidly. Such behavior has been correlated by terms similar to the last one in eq. 1. Therefore, following approximation for apparent molar heat capacity parameters $X(T)$ is proposed

$$T^2 X(T) = {T_0}^2 X_0 [1 - n/(T_0 - T_R) + n/(T - T_R)] \quad (10)$$

where X_0 is the value of the parameter at T_0 = 298.15 K and T_R = 263 K. The curves in Fig. 1b were calculated with $n = 28$ for $\beta^{(0)J}$ and C^J, and $n = 14$ for $\beta^{(1)J}$. At the present stage, it is unclear whether these two parameter values can be applied to other electrolytes as well, but it seems that this is a promising starting point for further investigations.

Instead of using a constant C_{p2}° value for 25 °C, it might be advantageous to combine eq. 10 with a $C_{p2}^\circ(T)$ function predicted with the revised HKF equation.

APPLICATION TO AQUEOUS SODIUM CARBONATE

Hydrolysis constant

The hydrolysis of the carbonate ion

$$CO_3^{2-} + H_2O \Leftrightarrow HCO_3^- + OH^- \quad (11)$$

is of both practical and theoretical interest. In the latter context, it leads, for example, to the "relaxation effect" observed during the measurement of apparent molar heat capacities at low concentrations, cf. the discussion and references given in [9]. In some practical applications, the influence of equilibrium (eq. 11) on the densities of sodium carbonate solutions cannot be neglected, especially at higher temperatures.

The equilibrium constant of reaction 11 can be obtained by combining the second dissociation constant of carbonic acid and the ionic product of water. Both quantities have been measured at temperatures up to 250 °C and in NaCl media up to 5 mol kg^{-1} in ionic strength [18,19]. Figures 2a and 2b compare these data with predictions from the CHC model [7]. Figure 2a shows a very good agreement

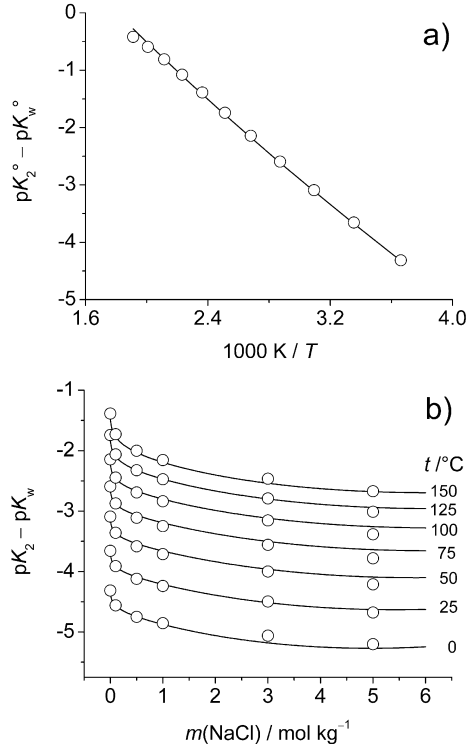

Fig. 2 Hydrolysis constant of carbonate, (a) at infinite dilution, **(b)** in NaCl media. Experimental data: circles [18,19]. Solid lines, calculated from the CHC model with data of ref. [7].

for the hydrolysis constant at infinite dilution to at least 225 °C (it has been noted in ref. [19] that plots of log K vs. $1/T$ are in general close to linear for such reactions). In NaCl media, the hydrolysis constant is well represented by the model of ref. [7] to about 150 °C (Fig. 2b). The curves in Fig. 2b have been conveniently calculated with ChemSheet [5].

Phase diagram

The Na_2CO_3–H_2O phase diagram calculated according to the CHC model of ref. [7] was extended to higher temperatures to include the anhydrous Na_2CO_3(s) phase (Fig. 3). The ChemSage optimizer was used to fit $\Delta_f H^\circ_{298} = -(1126.9 \pm 1.5)$ kJ mol^{-1} and $S^\circ_{298} = (140.6 \pm 3.9)$ J mol^{-1} K^{-1} to experimental solubility data [20]. These values differ from calorimetrically determined quantities ($\Delta_f H^\circ_{298} = -(1129.18 \pm 0.26)$ kJ mol^{-1}, $S^\circ_{298} = (134.98 \pm 0.84)$ J mol^{-1} K^{-1}) [21] by about 2σ, thus indicating that the thermodynamic data for solid and aqueous phases become increasingly inconsistent at higher temperatures.

It should be noted that it is extremely difficult to model solubilities that change only very slightly with temperature, as rather small changes in the heat capacity or relative enthalpy of the solution have a comparatively large effect on the temperature coefficient of solubility. Thus, the calculated solubilities of Na_2CO_3 phases at higher temperatures are quite reasonable, given that the simple CHC model has been used for the aqueous phase.

The dotted lines in Fig. 3 were calculated according to model 10 for temperature-dependent heat capacities as proposed in this work. The values of the parameter n derived above for NaCl(aq) were employed for both Na_2CO_3(aq) and $NaHCO_3$(aq). Standard partial molar heat capacities of

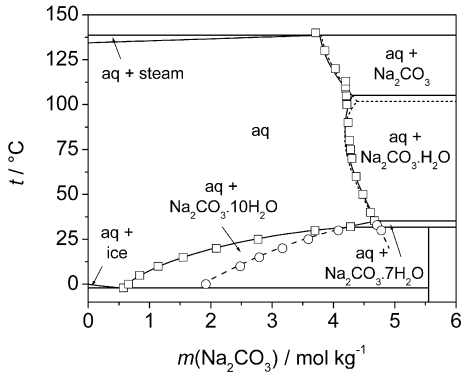

Fig. 3 Temperature-composition phase diagram of the Na_2CO_3–H_2O system at P = 3.02 atm. Experimental data: squares, stable equilibria; circles, metastable equilibria [20]. Solid and dashed lines, indicating stable and metastable equilibria, respectively, were calculated from the CHC model; dotted lines, model according to eq. 10, see text.

Na_2CO_3(aq) and $NaHCO_3$(aq) were calculated with SUPCRT92 {the 25 °C value for Na_2CO_3(aq) was slightly adjusted in accordance with ref. [9]}. The model for the apparent molar heat capacities of Na_2CO_3(aq) at 25 °C was based on the most recent measurements [9]. The calculated phase diagram looks reasonable up to ca. 140 °C. The values of $\Delta_f H°_{298}$ and $S°_{298}$ for Na_2CO_3(s), which were fitted to solubility data, are closer to the quantities reported in ref. [21] than those determined in conjunction with the CHC model (see above). However, calculated solubilities deviate significantly from experimental values above 150 °C, indicating increasing inconsistencies at these temperatures.

Relative apparent molar enthalpies

Polya et al. [22] have recently measured molar enthalpies of dilution of Na_2CO_3(aq) between m = 0.008 mol kg^{-1} and m = 1.45 mol kg^{-1} at temperatures from T = 298 K to T = 523 K at pressures of P = 7 MPa and P = 40 MPa. Polya et al. correlated their data by a Pitzer model with parameters for 298.15 K taken from ref. [23]. In addition, they derived 13 enthalpy parameters for each pressure.

Figure 4a shows relative apparent molar enthalpies of Na_2CO_3(aq) at P = 1 bar [22] compared to values calculated according to (i) the CHC model [7] and (ii) model (10) for temperature-dependent heat capacities proposed as described above. The agreement with the experimental relative apparent molar enthalpy values is clearly improved, although a discrepancy that increases with temperature still remains.

Figure 4a demonstrates the dangers inherent in the Pitzer model with respect to extrapolations outside the parameterization space. The dotted line, calculated according to the model of ref. [22], shows an upturn at m > 1.45 mol kg^{-1}, which not only disagrees with other enthalpy measurements [24] but also leads to completely incorrect solubility predictions. It is, thus, very important that models for solubility calculations are parameterized up to saturation (or even beyond when supersaturated solutions can be investigated).

Apparent molar heat capacities

The model according to eq. 10, as described in the previous section, was used to calculate apparent molar heat capacities of Na_2CO_3(aq) between 25 °C and 50 °C (Fig. 4b). The ${}^{\phi}C_p$ data of refs. [25,26] were measured by static calorimetry. It is difficult to assess their accuracy at higher temperatures, but it can be seen from Fig. 4b that the 25 °C data agree well with values measured recently with a Picker

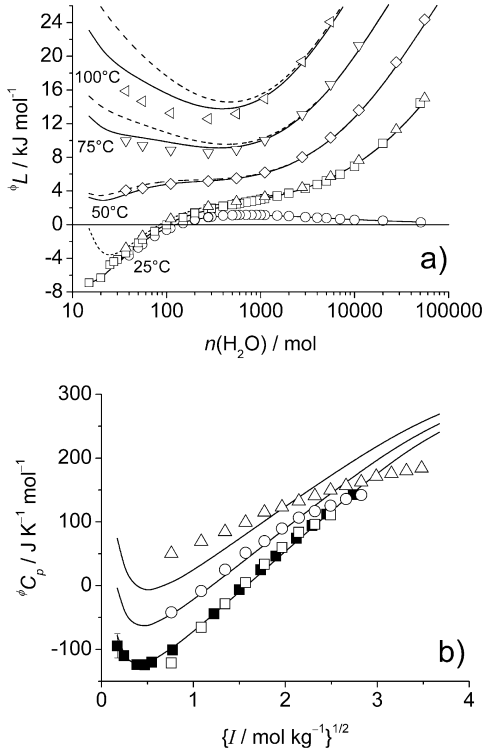

Fig. 4 (a) Relative apparent molar enthalpies of Na_2CO_3(aq) at P = 1 bar. Experimental data: squares [24]; circles, corrected for hydrolysis [24]; all other symbols [22]. Dashed lines, CHC model [7]; solid lines, temperature-dependent heat capacity parameters according to eq. 10; dotted line, Pitzer parameters of ref. [22]. (b) Apparent molar heat capacities of Na_2CO_3(aq). Experimental data: squares, 25 °C; circles, 35 °C; triangles, 50 °C; filled symbols [9]; open symbols [25,26]. Lines were calculated according to model 10 as explained in the text.

flow calorimeter [9]. It should be noted that the upturn in the $^{\phi}C_p$ values at low molalities results from the "relaxation effect" mentioned earlier.

It was possible to achieve almost perfect agreement with these experimental values by fitting a heat capacity model with different temperature dependence to the data (not shown). However, it turned out that this model is inconsistent with the temperature dependence of apparent molar enthalpy data of ref. [22]. To reproduce experimental solubility data satisfactorily, this model also requires thermodynamic quantities of solids, especially of Na_2CO_3(s), that are inconsistent with calorimetrically determined values [21].

Volumetric properties

Krumgalz et al. [27] have reviewed the literature on low-temperature density data for Na_2CO_3(aq) and $NaHCO_3$(aq) and have derived volumetric Pitzer models valid from 15 to 60 °C and 5 to 45 °C, respectively. To represent the standard partial molar volumes and volumetric Pitzer parameters, Krumgalz et al. have used a power series in temperature. Such functions generally have poor extrapolative capabilities, as can be seen from the dotted lines in Figs. 5a and 5b.

Sharygin and Wood [28] have measured densities of Na_2CO_3(aq) and $NaHCO_3$(aq) between m = 0.1 mol kg^{-1} and m = 1.0 mol kg^{-1} at temperatures from T = 298 K to T = 623 K and pressures

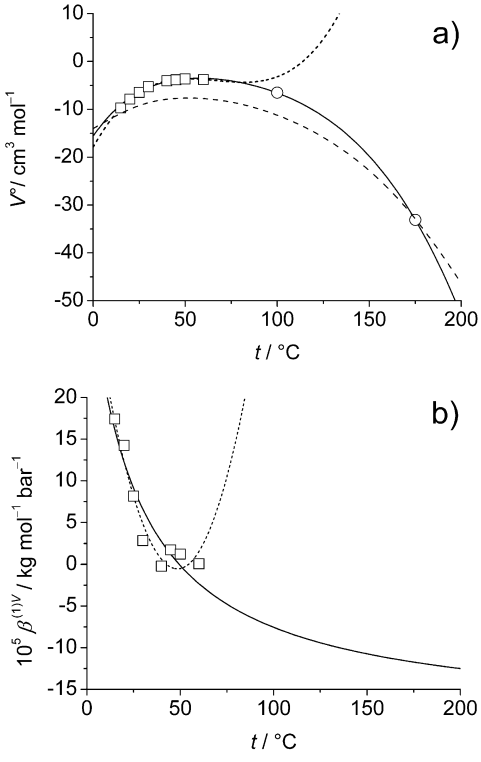

Fig. 5 (a) Standard partial molar volume and (b) $\beta^{(1)V}$ parameter of Na_2CO_3(aq). Squares and dotted line, values and functions, respectively, from ref. [27]. Circles, values obtained by extrapolation to $I = 0$ of data reported by [28]. Solid lines, temperature functions proposed in this study, dashed line, SUPCRT92 [12].

of $P = 10$ MPa and $P = 28$ MPa. Their data have been used in this work to extend the model of ref. [27] to higher temperatures and pressures. Thereby, only the standard partial molar volumes of Na_2CO_3(aq) and $NaHCO_3$(aq) were treated as pressure dependent, while the volumetric Pitzer parameters were not. For the standard partial molar volumes, temperature functions similar to eq. 1 were used (Fig. 5a). In analogy to the volumetric Pitzer parameters for NaCl(aq) [11], a temperature dependence similar to eq. 10 was assumed for the $\beta^{(1)V}$ parameter of Na_2CO_3(aq), which is shown as an example in Fig. 5b.

The hydrolysis of carbonate and its influence on Na_2CO_3(aq) densities are taken into account. Figures 6a and 6b show that apparent molar volumes are well represented to at least 175 °C. It should be noted that the HKF (SUPCRT92) predictions for $V°$ deviate significantly from the values chosen for the present model (Fig. 5a).

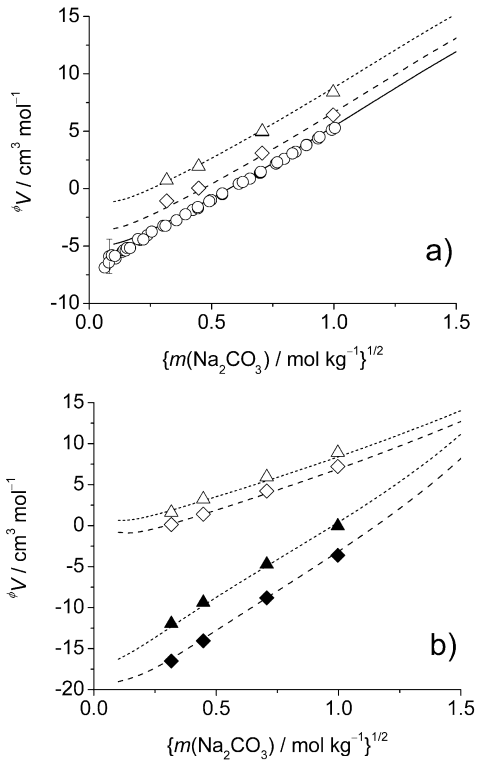

Fig. 6 Apparent molar volumes of Na_2CO_3(aq), (a) at 25 °C, (b) at 100 °C (open symbols) and 175 °C (filled symbols). Experimental values: circles, 1 bar [29]; diamonds, 100 bar [28], triangles, 280 bar [28]. The lines were calculated according to the present Pitzer model.

CONCLUSION

Thermodynamically consistent evaluations, based on various kinds of data measured over wide ranges of temperature, pressure, and concentration (up to saturation), have been reported only for very few electrolyte systems. For the majority of systems, data are only available for 25 °C. In these cases, the CHC model [7] or its extension (eq. 10) can be used to generate a temperature-dependent model that is valid to ca. 100 °C.

There are intermediate cases for which a few sets of different kinds of data have been measured over limited ranges of conditions. Usually, inconsistencies exist among these data sets, as have been identified in this work for Na_2CO_3(aq). The strategies outlined in this work might help to derive thermodynamically consistent models for such systems.

Thermodynamically consistent electrolyte models are a prerequisite for the simulation and the optimization of hydrometallurgical processes. For such simulations, ChemApp can be favorably used as has been demonstrated recently for the $Na_2SO_4 \rightarrow K_2SO_4$ conversion [30]. Process operations like heating, cooling, dissolution, precipitation, evaporation, etc. have been coded in order to calculate the associated material streams and extensive property balances. A new feature of ChemApp permits the incorporation of any functional form for the model parameters as defined by the user. A library of such subroutines with reliable Gibbs energy models for water, steam, and various electrolytes has been developed.

The simulation of other industrially relevant hydrometallurgical processes is currently under investigation.

REFERENCES

1. G. Eriksson and K. Hack. *Metall. Trans. B* **21B**, 1013 (1990).
2. C. W. Bale and A. D. Pelton. *FACT-Win – User Manual*, CRCT, École Polytechnique de Montréal, Québec, Canada, http://www.crct.polymtl.ca (1999).
3. E. Königsberger and G. Eriksson. *CALPHAD* **19**, 207 (1995).
4. G. Eriksson, K. Hack, S. Petersen. *ChemApp—A Programmable Thermodynamic Calculation Interface*. http://gttserv.lth.rwth-aachen.de/~sp/tt/abstract/eri97.htm (1997).
5. P. Koukkari, K. Penttilä, K. Hack, S. Petersen. *ChemSheet—an Efficient Worksheet Tool for Thermodynamic Process Simulation*. http://gttserv.lth.rwth-aachen.de/~sp/tt/abstract/kou00.htm (2000).
6. L. Kaufman and H. Bernstein. *Computer Calculation of Phase Diagrams,* Academic Press, New York (1970).
7. E. Königsberger. *Monatsh. Chem*. **132**, 1363 (2001).
8. K. S. Pitzer. In *Activity Coefficients in Electrolyte Solutions*, K. S. Pitzer (Ed.), 2nd ed., p. 75, CRC Press, Boca Raton, FL (1991).
9. M. C. F. Magalhães, E. Königsberger, P. M. May, G. Hefter. *J. Chem. Eng. Data* **47**, 590 (2002).
10. M. C. F. Magalhães, E. Königsberger, P. M. May, G. Hefter. *J. Chem. Eng. Data* **47**, 960 (2002).
11. K. S. Pitzer, J. C. Peiper, R. H. Busey. *J. Phys. Chem. Ref. Data* **13**, 1 (1984).
12. J. M. Johnson, E. H. Oelkers, H. C. Helgeson. *Comput. Geosci.* **18**, 899 (1992).
13. H. C. Helgeson and D. H. Kirkham. *Am. J. Sci.* **276**, 97 (1976).
14. J. Sedlbauer, J. P. O'Connell, R. H. Wood. *Chem. Geol.* **163**, 43 (2000).
15. G. Meinrath. *Fresenius J. Anal. Chem.* **368**, 574 (2000).
16. D. J. Bradley and K. S. Pitzer. *J. Phys. Chem.* **83**, 1599 (1979).
17. A. D. Pelton. Personal communication (2000).
18. R. H. Busey and R. E. Mesmer. *J. Chem. Eng. Data* **23**, 175 (1978).
19. C. S. Patterson, R. H. Busey, R. E. Mesmer. *J. Solution Chem*. **13**, 647 (1984).
20. W. F. Linke and A. Seidell. *Solubilities*, *Inorganic and Metal-Organic Compounds*, Vol. 2, American Chemical Society, Washington, DC (1965).
21. C. E. Vanderzee. *J. Chem. Thermodyn*. **14**, 219 (1982).
22. D. A. Polya, E. M. Woolley, J. M. Simonson, R. E. Mesmer. *J. Chem. Thermodyn*. **33**, 205 (2001).
23. J. C. Peiper and K. S. Pitzer. *J. Chem. Thermodyn*. **14**, 613 (1982).
24. R. L. Berg and C. E. Vanderzee. *J. Chem. Thermodyn*. **10**, 1049 (1978).
25. E. I. Chernen'kaya. *Zh. Prikl. Khim*. **44**, 1543 (1971).
26. E. I. Chernen'kaya and E. G. Bratash. *Zh. Prikl. Khim*. **45**, 2218 (1972).
27. B. S. Krumgalz, R. Pogorelsky, A. Sokolov, K. S. Pitzer. *J. Phys. Chem. Ref. Data* **29**, 1123 (2000).
28. A. V. Sharygin and R. H. Wood. *J. Chem. Thermodyn*. **30**, 1555 (1998).
29. J. T. Hershey, S. Sotolongo, F. J. Millero. *J. Solution Chem*. **12**, 233 (1983).
30. E. Königsberger and G. Eriksson. *J. Solution Chem*. **28**, 721 (1999).